Origins of Apparent Fragile-to-Strong Transitions of Protein Hydration Waters

M. Vogel

Institut für Festkörperphysik, Technische Universität Darmstadt, Hochschulstr. 6, 64289 Darmstadt, Germany

(Received 10 June 2008; published 26 November 2008)

^{2}H NMR is used to study the mechanisms for the reorientation of protein hydration water. In the past, crossovers in temperature-dependent correlation times were reported at $T_{x1} \approx 225$ K (X_1) and $T_{x2} \approx 200$ K (X_2). We show that neither X_1 nor X_2 are related to a fragile-to-strong transition. Our results rule out an existence of X_1. Also, they indicate that water performs thermally activated and distorted tetrahedral jumps at $T < T_{x2}$, implying that X_2 originates in an onset of this motion, which may be related to a universal defect diffusion in materials with defined hydrogen-bond networks.

DOI: 10.1103/PhysRevLett.101.225701 PACS numbers: 64.70.pm, 76.60.Lz, 87.15.kr

Studying the temperature dependence of the structural relaxation, one can distinguish ''strong'' and ''fragile'' glass-forming liquids, which do and do not show Arrhenius behavior, respectively [1]. For supercooled bulk water, it was proposed that a fragile-to-strong transition (FST) exists at about 225 K [2,3]. However, inevitable crystallization interferes with direct observation [4]. In confinement, crystallization can be avoided so that the dynamics of supercooled water are accessible down to the glass transition temperature T_g. For confined water, crossovers in the T dependence of a correlation time τ were observed at $T_{x1} \approx 225$ K (X_1) and $T_{x2} \approx 200$ K (X_2) using quasielastic neutron scattering (QENS) [5,6] and dielectric spectroscopy (DS) [7,8], respectively. Several workers took X_1 and X_2 as indications for a FST [5,6]. Also, X_1 was related to a liquid-liquid phase transition [5,6,9,10]. Challenging these conclusions, others argued that the Arrhenius processes P_1 and P_2 observed below X_1 and X_2, respectively, are secondary (β) relaxations [11,12], while structural (α) relaxation is difficult to observe [8].

Confined waters are of enormous importance for biological, geological, and technological processes; e.g., an interplay of water and protein dynamics enables biological functions [13]. Here, we investigate the hydration waters of elastin (E) and collagen (C), two proteins of the connective tissue. Using ^{2}H NMR, we study time scale and mechanism of water reorientation during T_{x1} and T_{x2}. The results show that a FST does not exist, while tetrahedral jumps become important upon cooling.

In ^{2}H NMR, the quadrupolar frequency is probed [14]:

$$\omega_Q(\theta, \phi) = \pm \frac{\delta}{2}(3\cos^2\theta - 1 - \eta\sin^2\theta\cos 2\phi). \quad (1)$$

Here, the angles (θ, ϕ) describe the orientation of the electric field gradient (EFG) tensor at the nuclear site with respect to the external static magnetic field. Since the molecular orientation determines the orientation of the EFG tensor, rotational jumps render ω_Q time dependent. The anisotropy and asymmetry of the tensorial interaction are characterized by δ and η, respectively. The $\pm$ signs correspond to two allowed transitions between three Zeeman levels of the ^{2}H nucleus ($I = 1$).

C, E, and D_2O were purchased from Aldrich. Weighed amounts of protein and D_2O were carefully mixed and sealed in the NMR tube to prepare samples with hydration levels $h = 0.25$–0.96 (g D_2O/1 g protein). We refer to the samples as ''E'' or ''C'' followed by the value of h in percent. ^{2}H NMR spin-lattice relaxation (SLR), line shape (LS), and stimulated-echo (STE) measurements are performed at a Larmor frequency of $\omega_L = 2\pi \times 76.8$ MHz. The experimental setup is described in Ref. [15].

In the studied samples, supercoolable bound water and freezable free water can coexist. Furthermore, deuterons replace exchangeable hydrogens of the protein [16]. On the basis of the amino acid compositions [17], one expects 10%–30% of the deuterons to be bound to proteins for the used hydration levels. Hence, deuterons of supercooled water, crystalline water, and protein can contribute to ^{2}H NMR signals. Accordingly, three steps are observed in SLR measurements for $C60$; see Fig. 1(a). The third step results from deuterons of crystalline water, as can be inferred from its absence for low hydration levels, e.g., for $C25$, when free water does not exist [18–20]. Since water deuterons outnumber protein deuterons, the higher first and lower second steps can be assigned to supercooled water and protein, respectively. The existence of distinct

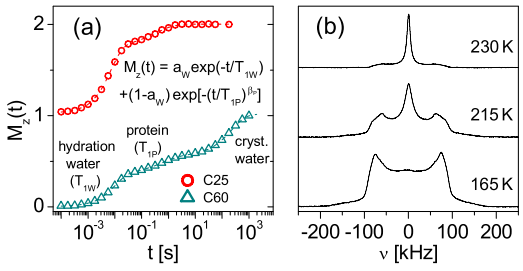

FIG. 1 (color online). (a) Buildup of the magnetization $M_z(t)$ after saturation for $C25$ at 230 K (shifted) and $C60$ at 235 K together with fits to two- and three-step relaxations, respectively. The two-step fitting function is indicated. (b) T-dependent spectra of $E43$ from the solid-echo sequence, $90_x°$-Δ-$90_y°$-Δ-t.

steps means that deuteron exchange between the three species is slow on the time scale of SLR [16], enabling separate analysis of the dynamical behaviors in ^{2}H NMR.

Depending on the value of h, we use two- or three-step relaxations to fit the buildup of magnetization, $M_z(t)$; see Fig. 1(a). While we will not discuss results for crystalline water, Fig. 2(a) compares the T-dependent SLR times T_{1w} and T_{1p} of deuterons in supercooled waters and proteins, respectively. T_{1w} shows a very similar minimum for all samples, indicating that water dynamics in the hydration shells of C and E are highly comparable. Unlike the first step, the second step is nonexponential ($\beta_p \approx 0.6$), typical of amorphous solids [14]. For C and E, T_{1p} and, thus, the protein dynamics weakly depend on T.

Using that reorientation of the hydration waters is basically isotropic in the vicinity of the minimum, see below, T_{1w} depends on the spectral density according to [14]

$$T_{1w}^{-1} = (2/15)\delta^2[J(\omega_L) + 4J(2\omega_L)]. \quad (2)$$

Here, $J(\omega) = \int_0^\infty F_2(t)\cos(\omega t)dt$. The rotational correlation function (RCF) $F_2(t) \propto \langle P_2[\cos\theta(0)]P_2[\cos\theta(t)]\rangle$ describes the time dependence of the Legendre polynomial P_2 of the angle θ. For a Debye process, $F_2(t) = \exp(-t/\tau)$ and $J_{\mathrm{BPP}}(\omega) = \tau/(1 + \omega^2\tau^2)$. In this case, Eq. (2) takes the form derived by Bloembergen, Purcell, and Pound (BPP) [21]. This approach predicts $T_{1w} = 2.4$ ms at the minimum, at variance with our results in Fig. 2(a). Thus, a Debye process does not describe the water dynamics, but a distribution of correlation times $G(\log\tau)$ exists, as typical of supercooled liquids. To consider such distribution, Cole-Davidson (CD) and Cole-Cole (CC) spectral densities proved useful in SLR analyses [14,22]

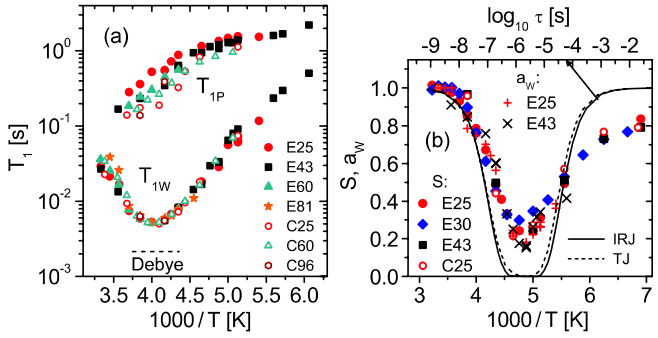

FIG. 2 (color online). (a) SLR times T_{1w} and T_{1p} for deuterons of supercooled waters and proteins, respectively. The dashed horizontal line is the expectation for the T_{1w} minimum in the case of a Debye process, as calculated from Eq. (2) for the experimental values $\delta = 2\pi \times 168$ kHz and $\omega_L = 2\pi \times 76.8$ MHz. (b) T-dependent integrated intensity S of solid-echo spectra and relative height a_w of the first SLR step for hydrated E and C samples. The lines show the dependence of S on the correlation time τ, as obtained in simulations of isotropic random jumps (IRJ) and tetrahedral jumps (TJ), using the experimental values $\delta = 2\pi \times 168$ kHz, $\eta = 0.1$, and $\Delta = 20$ μs.

$$J_{\mathrm{CD}}(\omega) = \omega^{-1}\sin[\beta_{\mathrm{CD}}\arctan(\omega\tau_{\mathrm{CD}})]/(1 + \omega^2\tau_{\mathrm{CD}}^2)^{(\beta_{\mathrm{CD}}/2)},$$

$$J_{\mathrm{CC}}(\omega) = \frac{\omega^{-1}\sin(\frac{\beta_{\mathrm{CC}}\pi}{2})(\omega\tau_{\mathrm{CC}})^{\beta_{\mathrm{CC}}}}{1 + (\omega\tau_{\mathrm{CC}})^{2\beta_{\mathrm{CC}}} + 2\cos(\frac{\beta_{\mathrm{CC}}\pi}{2})(\omega\tau_{\mathrm{CC}})^{\beta_{\mathrm{CC}}}}.$$

Employing J_{CD} (J_{CC}), a width parameter $\beta_{\mathrm{CD}} = 0.22$ ($\beta_{\mathrm{CC}} = 0.50$) is obtained from T_{1w} at the minimum. Assuming that β_{CD} (β_{CC}) is independent of T and inserting J_{CD} (J_{CC}) into Eq. (2), τ_{CD} (τ_{CC}) is extracted from T_{1w}. The mean correlation time $\langle\tau_{\mathrm{CD}}\rangle = \tau_{\mathrm{CD}}\beta_{\mathrm{CD}}$ [22] of the asymmetric CD distribution and the peak position τ_{CC} of the symmetric CC distribution are shown for $E25$ and $E43$ in Fig. 3(c). At 220–260 K, J_{CD} and J_{CC} yield comparable results, demonstrating insensitivity to the choice of the specific spectral density in this range. At lower T, non-Arrhenius and Arrhenius ($E_a = 0.60$ eV) behaviors are obtained from use of J_{CD} and J_{CC}, respectively, so that ambiguity about $J(\omega)$ hampers analysis. Anyhow, neither J_{CD} nor J_{CC} yield evidence that X_1 exists.

In the following, we focus on $h \leq 0.25$–0.43. Then, the hydration shells are fully occupied, while freezable water hardly exists [18,20]. In Fig. 1(b), we see that the solid-echo spectra of $E43$ are comprised of two components. Independent of T, the protein component is given by a broad spectrum, which is the typical LS in the absence of

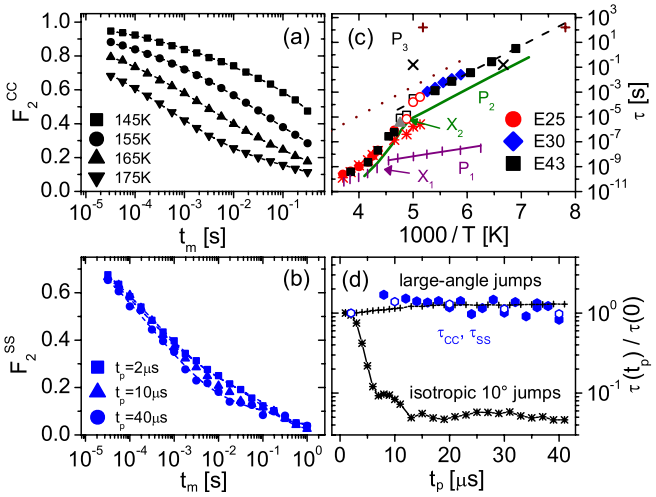

FIG. 3 (color online). (a) $F_2^{cc}(t_m; t_p = 30\ \mu\mathrm{s})$ of $E43$ at various T and fits to Eq. (4). (b) $F_2^{ss}(t_m; t_p = 2, 10, 40\ \mu\mathrm{s})$ of $E30$ from PR experiments at 185 K and fits to Eq. (4). (c) Correlation times from LS (triangle) and SLR analysis at $T \geq 195$ K (J_{CD}: circles and squares, J_{CC}: stars) and from STE analysis below 195 K [$E43$: $\langle\tau_{cc}\rangle$ from $F_2^{cc}(t_m; t_p = 30\ \mu\mathrm{s})$, $E30$: $\langle\tau_{ss}\rangle$ from PR $F_2^{ss}(t_m; t_p = 2\ \mu\mathrm{s}) \approx F_2(t_m)$]. Open symbols mark differing SLR results from J_{CD} and J_{CC}. Correlation times from measurements using DS for (solid line) hydrated myoglobin [31] and (dotted line) E ($h = 0.1$) [19], (+) TSC for E ($h = 0.5$) [20], (×) MR for C ($h \geq 0.5$) [18], and (|) QENS for hydrated lysozyme [6]. (d) Evolution-time dependence of $\langle\tau_{cc}\rangle$ (solid circles) and $\langle\tau_{ss}\rangle$ (open circles) from PR STE experiments on $E30$ at 185 K and simulation results for (+) distorted (±3°) tetrahedral jumps and (*) isotropic 10° jumps.

motion [14]. For the water component, this LS is observed at low T, but the broad spectrum collapses between 185 and 215 K resulting in a narrow Lorentzian at high T. The narrow spectrum reveals that, at $T \geq 215$ K, the water molecules show fast ($\tau \ll 1/\delta$) isotropic jumps that average out the anisotropy of the quadrupolar interaction, while anisotropic motions, e.g., π flips, do not result in a Lorentzian and can be excluded. At $T \leq 185$ K, the broad spectrum indicates that significant water dynamics is absent on the time scale of $1/\delta \approx 1$ μs. Thus, P_1, found in QENS works below T_{x1} [5,6], is not the α process so that X_1 is not a FST. If P_1 were the α process, a narrow Lorentzian would be observed as ^{2}H LS down to about 140 K due to $\tau_{P1} \ll 1/\delta$; see Fig. 3(c), in clear contrast to the findings in Fig. 1(b). The assignment and shape of the lines are confirmed when we single out the water contribution in partially relaxed (PR) experiments (not shown), in which we do not wait for complete recovery of M_z after saturation, but start acquisition at times between first and second SLR steps.

The total spectral intensity S, determined by integrating the solid-echo spectra after correction for the Curie factor, exhibits a minimum $S \approx 0.25$ at $T \approx 210$ K, see Fig. 2(b), indicating that water dynamics during the dephasing and rephasing periods Δ of the solid-echo sequence interferes with echo formation [23]. Random-walk simulations [24] for various motional models show that S is a minimum at $\tau = 3$ μs. The signal is not reduced for much faster (slower) dynamics, when ω_Q is time-averaged (time-invariant). Deviations between measured and calculated data result because the simulations do not consider a distribution $G(\log\tau)$ and protein contributions. In Fig. 3(c), we see that LS and SLR analyses yield consistent correlation times. In SLR experiments, the height a_w of the step due to supercooled water is also a minimum at 210 K since a solid echo is used; see Fig. 2(b).

Finally, we perform STE experiments [14] to study water dynamics at $T < T_{x2}$. In STE experiments, we correlate the instantaneous quadrupolar frequencies ω_Q of a deuteron during two short evolution times $t_p \ll \tau$ that are separated by a longer mixing time $t_m \approx \tau$. Using appropriate pulse sequences, variation of t_m for constant t_p enables measurement of RCF ($\xi = \sin, \cos$; $x = ss, cc$)

$$F_2^x(t_m; t_p) \propto \langle \xi[\omega_Q(0)t_p]\xi[\omega_Q(t_m)t_p]\rangle. \quad (3)$$

The brackets $\langle \ldots \rangle$ denote the ensemble average. F_2^{ss} and F_2^{cc} result for $\xi = \sin$ and $\xi = \cos$, respectively [14]. The RCF decay when slow ($t_p \approx 10$ μs $\leq \tau \leq T_1 \approx 1$ s) molecular reorientation alters the value of ω_Q during t_m.

Figure 3 presents $F_2^x(t_m; t_p)$ of $E30$ and $E43$. Water dynamics lead to decays at short times (Φ_w), while SLR results in additional damping of the water (R_w) and protein (R_p) contributions at longer times. Taking R_w and R_p from the above SLR analysis, we fit $F_2^x(t_m)$ to

$$A_w[(1 - B)\Phi_w(t_m) + B]R_w(t_m) + (1 - A_w)R_p(t_m). \quad (4)$$

Here, B is introduced to consider that water dynamics does not destroy all orientational correlation, see below. Using a stretched exponential $\Phi_w(t_m) = \exp[-(t_m/\tau)^\beta]$, we obtain stretching parameters $\beta = 0.27$–0.28 [25] for all studied values of t_p and T. Thus, hydration water exhibits strongly nonexponential RCF below 200 K. Use of the Γ function enables calculation of the mean correlation time, $\langle\tau\rangle = (\tau/\beta)\Gamma(1/\beta)$. In Fig. 3(c), we see that $\langle\tau_{ss}\rangle$ and $\langle\tau_{cc}\rangle$ from F_2^{ss} of $E30$ and F_2^{cc} of $E43$, respectively, follow the same Arrhenius law (dashed line) with activation energy $E_a = 0.45$ eV. We note that F_2^{ss} of $E30$ was obtained in PR experiments to minimize the protein contribution, leading to $(1 - A_w) = 0.05$–0.10.

Comparison of our SLR, LS, and STE data implies a crossover in the T dependence of water dynamics in the vicinity of T_{x2}. Here, exact determination of a crossover temperature is hampered by a dependence on the choice of the spectral density used in SLR analysis. For an understanding of the origin of X_2, knowledge about the mechanism for water dynamics below T_{x2} is of particular importance. We exploit that the dependence of STE decays on the length of the evolution time has been shown [14,26] to yield valuable insights into the geometry of rotational motion since sensitivity to small changes of ω_Q and, thus, small angular displacements is higher for large t_p; see Eq. (3). An analysis of $\langle\tau_x(t_p)\rangle$ enables a determination of jump angles. While small-angle reorientation, results in a strong decrease of $\langle\tau_x(t_p)\rangle$, $\langle\tau_x\rangle$ is independent of t_p for large-angle reorientation [14]; see Fig. 3(d). Extraction of $\langle\tau_x(t_p)\rangle$ from $F_2^x(t_m; t_p)$ of $E30$ shows that a substantial dependence on t_p is absent, in harmony with results for $C25$ (not shown). Hence, below T_{x2}, water exhibits large-angle rather than small-angle reorientation typical of the α process [14]. In Fig. 3(b), we see that $F_2^{ss}(t_m; t_p)$ decays to a small, but finite plateau $B(t_p)$, see Eq. (4), before the onset of SLR. The plateau height depends on the geometry of the motion, e.g., $B(t_p \to \infty) = 1/n$ for a n-site jump [26]. Here, B decreases from 0.16 to 0.06 when t_p is extended from 2 to 40 μs, indicating that, though water reorientation is not isotropic, angular restrictions are not severe [26]. While exact two- ($B = 1/2$) or four-site ($B = 1/4$) jumps can be excluded, distorted tetrahedral jumps, which may be expected for a disordered hydrogen-bond network, are consistent with the data [26]. In ^{2}H STE work on ice I_h [27], a similar dependence $B(t_p)$ was shown to indicate that translational diffusion of water molecules via interstitial defects involves distorted ($\pm 3°$) large-angle reorientation between 7 O-D bond orientations in ice.

In summary, we exploited the capabilities of ^{2}H NMR to ascertain correlation times and mechanisms for the rotational motion of supercooled protein hydration waters. In the literature [5–12], it was a controversial issue to take crossovers X_1 and X_2 of temperature-dependent τ as evidence for a FST. Prerequisite for such interpretation of X_1 or X_2 is that the processes P_1 or P_2 below these crossovers are the α process. The present results, e.g., the LS at

145–185 K, rule out that P_1 is the α process and, hence, that X_1 at $T_{x1} \approx 225$ K is a FST. While a narrow spectrum would result if P_1 were the α process, a broad spectrum is observed. Our findings conflict with QENS [5,6] and ^{1}H NMR diffusion [28] studies, attributing X_1 to a FST. Further evidence against X_1 being a FST comes from extrapolation of $\tau_{P1}(T)$, which yields too small values $T_g < 100$ K. Also, a weak wave-vector dependence $\tau(Q)$ below X_1 [6] implies local rather than diffusive motion. Our results are consistent with the conjecture that P_1 is a β process [8,11,12], if the underlying motion is too restricted to be probed in ^{2}H NMR.

Exploiting the sensitivity of ^{2}H NMR to the mechanisms for water reorientation, we investigated the origin of X_2 at $T_{x2} \approx 200$ K, reported in DS work [8,11]. Above T_{x2}, SLR and LS analyses showed that water exhibits isotropic reorientation described by a broad distribution $G(\log\tau)$. Below T_{x2}, STE experiments indicate that water performs large-angle jumps, most probably distorted tetrahedral jumps, which follow an Arrhenius law with $E_a = 0.45$ eV. For P_2, DS work on water in various confinements [11] reported comparable $\tau_{P2}(T)$; see Fig. 3(c). Also, mechanical-relaxation (MR) and thermally-stimulated currents (TSC) studies found a process with similar values of τ [18,20]. Therefore, all these methods probe P_2. However, P_2 neither destroys all orientational correlation, see Fig. 3, nor affects rigidity [18]. Thus, P_2 is not the α process and X_2 is not a FST. Moreover, the large-angle jump mechanism is strong evidence against P_2 being a Johari-Goldstein β process [29], which results from small-amplitude reorientation [30]. Comparison with previous ^{2}H NMR work [27] showed that diffusion of water molecules via interstitial defects is consistent with the present results. Since $E_a \approx 0.45$ eV is not only found for water in various confinements [11], but also for crystalline and glassy bulk water [3], we suggest that water shows a characteristic tetrahedral jump motion, which is controlled by breaking of hydrogen bonds and, possibly, related to interstitial defect diffusion whenever a defined hydrogen-bond network is established, although we cannot exclude that the tetrahedral jump motion is governed by the protein surfaces in our case. The onset of this tetrahedral jump motion leads to more or less pronounced crossovers X_2. Extrapolating $\tau_{P2}(T)$, a value of 100 s is reached in the vicinity of 136 K, the first widely accepted [4], but later questioned [3] value of T_g for bulk water. Thus, one might speculate that the reported small calorimetric effects are not related to a glass transition, but to freezing of interstitial defects.

^{2}H NMR, which probes single-particle RCF, cannot resolve the issue whether the α process exists below X_2, because P_2 destroys basically all orientational correlation before an onset of structural relaxation. Detection of the α process rather requires techniques sensitive to the reorganization of the whole hydrogen-bond network. In this respect, it is interesting that MR and TSC studies [18,20] found a slower process P_3, see Fig. 3(c), which affects rigidity and, hence, may be the α process. Finally, it is an open question whether the onset of tetrahedral jump motion is related to a liquid-liquid phase transition, which was proposed to lead to a low-density liquid with a more ordered tetrahedral network upon cooling [3,4].

Funding of the DFG through Grants VO 905/3-1 and VO 905/3-2 is gratefully acknowledged.

[1] C. A. Angell, Science **267**, 1924 (1995).
[2] K. Ito, C. T. Moynihan, and C. A. Angell, Nature (London) **398**, 492 (1999).
[3] C. A. Angell, Science **319**, 582 (2008).
[4] O. Mishima and H. E. Stanley, Nature (London) **396**, 329 (1998).
[5] L. Liu *et al.*, Phys. Rev. Lett. **95**, 117802 (2005).
[6] S.-H. Chen *et al.*, Proc. Natl. Acad. Sci. U.S.A. **103**, 9012 (2006).
[7] R. Bergman and J. Swenson, Nature (London) **403**, 283 (2000).
[8] J. Swenson, H. Jansson, and R. Bergman, Phys. Rev. Lett. **96**, 247802 (2006).
[9] P. Kumar *et al.*, Phys. Rev. Lett. **97**, 177802 (2006).
[10] J.-M. Zanotti, M.-C. Bellissent-Funel, and S.-H. Chen, Europhys. Lett. **71**, 91 (2005).
[11] S. Cerveny *et al.*, Phys. Rev. Lett. **93**, 245702 (2004).
[12] S. Pawlus, S. Khodadadi, and A. P. Sokolov, Phys. Rev. Lett. **100**, 108103 (2008).
[13] P. W. Fenimore *et al.*, Proc. Natl. Acad. Sci. U.S.A. **101**, 14 408 (2004).
[14] R. Böhmer *et al.*, Prog. Nucl. Magn. Reson. Spectrosc. **39**, 191 (2001).
[15] M. Vogel and T. Torbrügge, J. Chem. Phys. **125**, 164910 (2006).
[16] G. E. Ellis and K. J. Packer, Biopolymers **15**, 813 (1976).
[17] N. Vyavahare *et al.*, Am. J. Pathology **155**, 973 (1999).
[18] S. Nomura *et al.*, Biopolymers **16**, 231 (1977).
[19] V. Samouillan *et al.*, Biomacromolecules **3**, 531 (2002).
[20] V. Samouillan *et al.*, Biomacromolecules **5**, 958 (2004).
[21] N. Bloembergen, E. M. Purcell, and R. V. Pound, Phys. Rev. **73**, 679 (1948).
[22] C. P. Lindsey and G. D. Patterson, J. Chem. Phys. **73**, 3348 (1980); P. A. Beckmann, Phys. Rep. **171**, 85 (1988).
[23] C. Schmidt, K. J. Kuhn, and H. W. Spiess, Prog. Colloid & Polymer Sci. **71**, 71 (1985).
[24] M. Vogel and E. Rössler, J. Magn. Reson. **147**, 43 (2000).
[25] Using $\beta = 0.97\beta_{\mathrm{CD}} + 0.14$; see Ref. [22], $\beta_{\mathrm{CD}} = 0.22$ from SLR analysis translates into $\beta = 0.35$.
[26] G. Fleischer and F. Fujara, *NMR-Basic Principles and Progress* (Springer, Berlin, 1994), Vol. 30, p. 159.
[27] B. Geil, T. M. Kirschgen, and F. Fujara, Phys. Rev. B **72**, 014304 (2005).
[28] F. Mallamace *et al.*, J. Chem. Phys. **127**, 045104 (2007).
[29] G. P. Johari and M. Goldstein, J. Chem. Phys. **53**, 2372 (1970).
[30] M. Vogel and E. Rössler, J. Chem. Phys. **114**, 5802 (2001).
[31] J. Swenson *et al.*, J. Phys. Condens. Matter **19**, 205109 (2007).